FATIGUE CRACK GROWTH PREDICTIONS IN RIVETED JOINTS

S. A. Fawaz
Air Force Research Laboratory
Wright-Patterson AFB, OH 45433, USA
(937) 255-6104 ext. 239
(937) 656-4999
scott.fawaz@flight.wpafb.af.mil

J. Schijve
Faculty of Aerospace Engineering, Delft University of Technology
Kluyverweg 3, 2629 HS Delft, The Netherlands

ABSTRACT

A characteristic aspect of fatigue of riveted lap joints is the occurrence of crack growth under a complex stress system, which in its simplest form consists of cyclic tension with superimposed cyclic bending due to the eccentricity in the lap joint. In reality, rivet squeezing leads to hole expansion and built-in residual stresses. In the empirical part of the investigation a simpler problem was analyzed first, i.e. fatigue crack growth in a multiple-hole sheet specimen loaded under combined tension and bending stress. Crack growth development for small part-through cracks could be followed by fractographic observations employing marker load cycles in between constant-amplitude loading. The same marking technique was employed for a simple lap joint having two rivet rows with four rivets in each row. The crack growth history could be reconstructed from a crack length of 75 μm to final fracture at 12 mm.

In the analytical part, the well-known Newman-Raju K-solutions are available for part-through cracks. After through cracks are obtained they continue to grow with oblique crack fronts due to the combined tension and bending. Since no K-solutions are available for these cracks, the finite-element method and a three dimensional virtual crack closure technique (3D VCCT) were adopted. K-solutions for the crack shapes obtained in the open hole sheet specimen lap joint experiments are then calculated and adopted for the prediction of the growth of these cracks. A satisfactory agreement has been obtained. K-values have been calculated for a range of crack depth to crack length ratios, crack depth to sheet thickness ratios, and hole radius to sheet thickness ratios.

The Newman/Raju K-solutions and newly calculated K-solutions for the through cracks have been incorporated into a crack growth prediction scheme. The prediction algorithm not only predicts the fatigue life within 6% of the actual life, but also accurately predicts the crack growth history until just prior to final fracture.

1. Introduction

The crack growth prediction model developed here does not use a new crack growth law or incorporate any new phenomenological behavior witnessed during the experimental investigation. Simply stated, the crack growth model predicts crack growth of part through and through cracks with crack shapes typically found in longitudinal lap-splice joints of pressurized fuselage structure. Results of fatigue crack growth experiments on different types of specimens are used for the validation of the prediction model. It covers, center cracked tension specimens, center cracked tension/bending specimens, specimens with a single open hole with edge cracks, and riveted lap joint specimens. In view of the aims of the present research program on fatigue of riveted lap joints of fuselage lap splices, the predictions are restricted to constant-amplitude (CA) loading, but it includes part through cracks with a quarter elliptical crack front as well as through cracks with an oblique crack front. Moreover, combined tension and bending is addressed.

The predictions are compared to results obtained in the experimental investigation. Stress intensity factors are partly borrowed from the literature. For the part through crack growth, the well-known Newman/Raju stress intensity factor equations are used. The through crack portion of the fatigue life is modeled using the newly developed stress intensity solutions for a part elliptical through crack shown in Figure 1 which was first presented in reference [1]. A question that immediately comes to mind is how to address the transition from a part through to through crack? The transition is supposed to occur at the moment that K at the deepest point along the bore of the hole exceeds 1.4 times K_{Ic}, which is the criterion used in the NASGRO Crack Growth Computer Program[3]. The crack depth then becomes equal to the sheet thickness. The smallest a/t ratio of a through crack for which K values became available from the FEA results is 1.05. This value is then used for calculating the first growth increment of the through crack after break through to the other sheet surface.

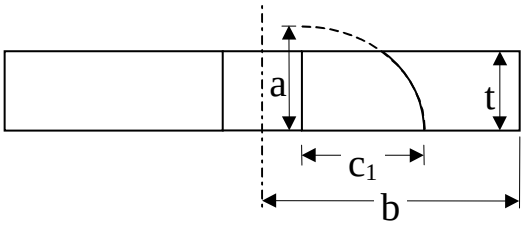

Figure 1 Part-Elliptical Through Crack Geometry

The sheet material considered is 2024-T3 Alclad. The basic da/dN - ΔK crack growth data used for predictions are presented first (section 2), followed by predictions for part through cracks in section 3 and oblique through cracks in section 4. Both types of cracks are considered under different types of loading. The investigation is summarized in a number of conclusions in section 5.

2. Basic da /dN -ΔK Relation Adopted for Crack Growth Predictions

The Forman-Newman-de Koning, FNK, crack growth equation is used to describe the basic da/dN - ΔK relation applicable to 2024-T3 thin sheet material. The FNK equation, Eqn. (1) is an extension of the Forman equation with added parameters, p and q, to better fit the material data in the extremal regions of the da/dN vs. ΔK curve.[2-4]

$$\frac{da}{dN} = C\left(\frac{1-f}{1-R}\Delta K\right)^n \frac{\left(1-\frac{\Delta K_{th}}{\Delta K}\right)^p}{\left(1-\frac{K_{\max}}{K_c}\right)^q} \tag{1}$$

where a = crack length, N = number of applied fatigue cycles, R = stress ratio, ΔK = stress intensity factor range, C, n, p, q = empirically derived material constants, f = crack opening function, ΔK_{th} = threshold stress intensity factor, K_c = critical stress intensity factor. The crack opening function, f, for plasticity induced crack closure, is defined by Newman as[5]

$$f = \frac{K_{op}}{K_{\max}} = \begin{cases} \text{maximum of } R \text{ or } A_0 + A_1 R + A_2 R^2 + A_3 R^2 & R \geq 0 \\ A_0 + A_1 R & -2 \leq R < 0 \end{cases} \tag{2}$$

with the A_i coefficients given below.

The plane stress/plane strain constraint factor is α and σ_{max} and σ_0 are the maximum applied stress and flow stress, respectively. For the predictions where the crack opening function is included, α is set to 1.5, as recommended in reference [3], and the ratio of σ_{max}/σ_o to 0.3.[3,5] Although the equations appear overly complicated for constant amplitude loading, it degenerates to the closure corrected Paris equation by setting p = q = 0. If the material does not exhibit significant crack closure, the crack opening function can be bypassed by setting f equal to R; i.e., $K_{op} = K_{min}$. In addition, if p and q are again set to zero, Eqn. (1)

$$A_0 = \left(0.825 - 0.34\alpha + 0.05\alpha^2\right)\left[\cos\left(\frac{\pi}{2}\frac{\sigma_{max}}{\sigma_0}\right)\right]^{\frac{1}{\alpha}}$$

$$A_1 = \left(0.415 - 0.071\alpha\right)\frac{\sigma_{max}}{\sigma_0}$$

$$A_2 = 1 - A_0 - A_1 - A_3$$

$$A_3 = 2A_0 + A_1 - 1$$

[12] and 3.07, respectively.

reverts to the Paris equation, $da/dN = C\Delta K^n$. A more in depth review of the FNK equation is presented in references [2-5]. The full equation has been coded in the computer program to give the user a choice of the three crack growth relations. For most predictions here, the Paris equation is used unless otherwise stated. From constant amplitude fatigue test data of center crack tension specimens, shown in Figure 2, the da/dN - ΔK relation is established, from which the Paris constants, C and n, are calculated to be $1.67 \times 10^{-}$

3. The Growth of Part Through Cracks

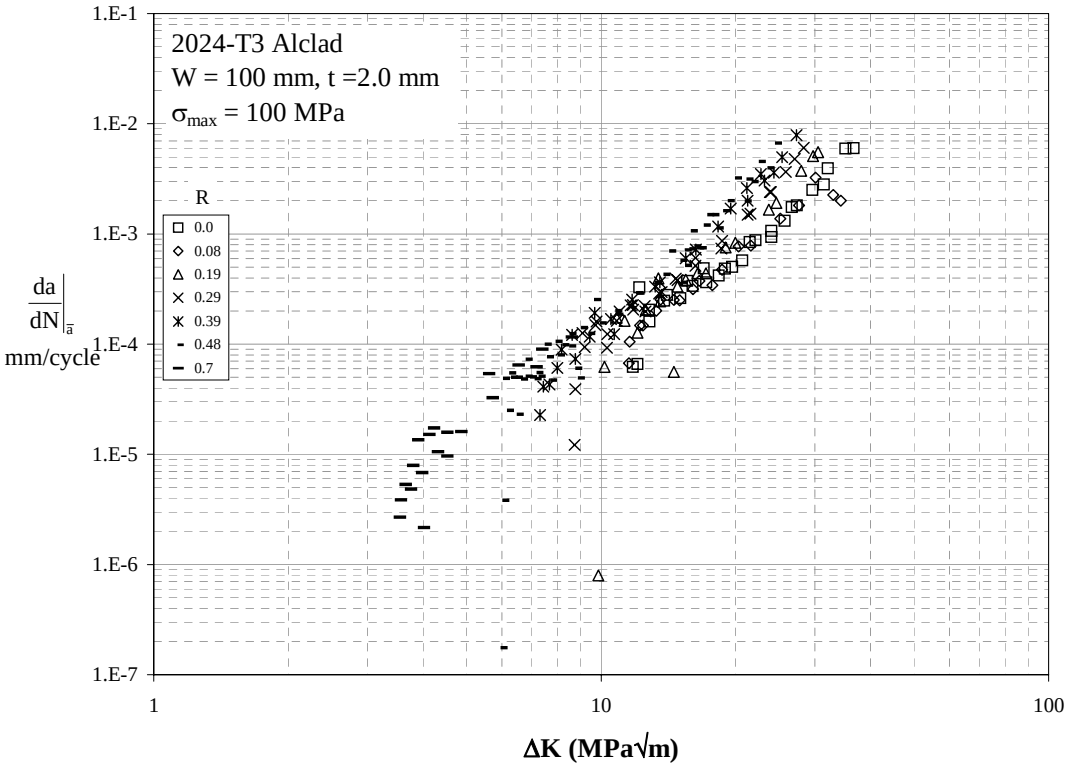

Figure 2 Crack Growth Rate Data Used for Predictions

Part through cracks initiated at the bore of a hole are generally supposed to have a quarter elliptical crack front. The size is then determined by the two semi-axis, the crack length "c_1" and the crack depth "a", see Figure 3. For the prediction of the fatigue crack growth life, an initial flaw assumption must be made, not only for the crack size, but also for the crack shape. For example, if the initial crack length "c_1" is assumed to be 1.27 mm (0.05 in., an initial crack size adopted by the USAF Damage Tolerance Requirements), an initial crack depth "a" must also be assumed. A parametric study is completed in section 3.1 to investigate the dependence of the part through crack growth on the assumed shape of the initial flaw. Predictions are made for the same value of "a" but three values of a/c_1 of the initial flaw. The predictions are based on calculating da/dN and dc_1/dN in order to find the new locations of the semi-axis of the quarter elliptical crack. It thus is assumed that the crack front remains quarter elliptical and that the prediction can be restricted to two points of the crack front. This is the approach generally

adopted in the literature. Predictions for crack extension are made in for a large number of points distributed along the crack front. A quarter ellipse is then drawn through the predicted new points of the crack front. For that purpose a regression analysis is used. In sections 3.1 and 3.2, sensitivity studies are completed to determine the effect of the initial flaw shape assumption and the bending factor, respectively. A comparison between predicted and observed crack shapes is made in section 3.3. It should be noted that the predictions in sections 3.1 – 3.3 are made for combined tension and bending.

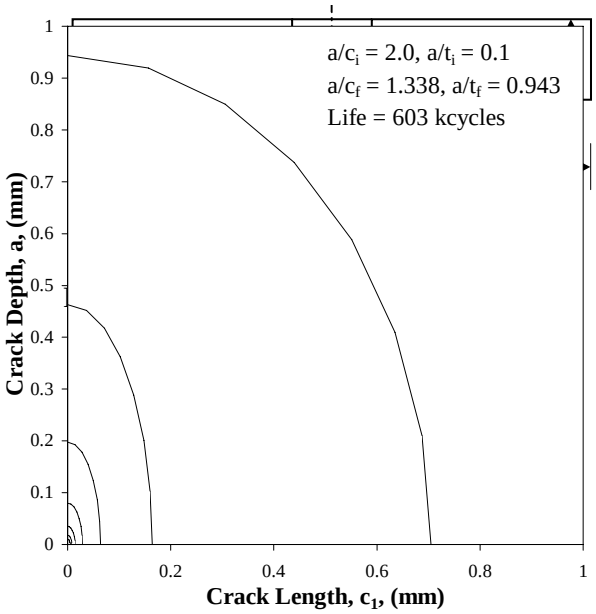

Figure 6 Crack Shape Development with Initial $a/c_1 = 2.0$

3.1 The Effect of the Initial Flaw Shape a/c_1

The Newman/Raju corner crack solutions for K-values remain as the primary reference for crack growth predictions of part elliptical crack geometries. For this reason, not to mention the ease of programming the numerous polynomial equations, the Newman/Raju solutions are the only solutions used for part through crack growth.[6] For the predictions that are completed here, the same initial crack depth is a = 0.01 mm, but there are three values of the a/c_1 ratio: 0.5, 1.0, and 2.0, i.e. c_1 = 0.02, 0.01, and 0.005 mm, respectively. The calculations are for a 100 mm wide specimen of 2024-T3, thickness 1.0 mm with a 2.0 mm hole in the center. The remote stress is 100 MPa of both tension and bending (bending factor k = 1.0). Obviously, the bending should affect the fatigue crack shape development. Results are shown in Figure 4 - Figure 6 for the three a/c_1 ratios, respectively. The figures show crack fronts obtained at intervals of approximately 20% of the fatigue life defined by the last crack front to static break through of the remaining ligament.

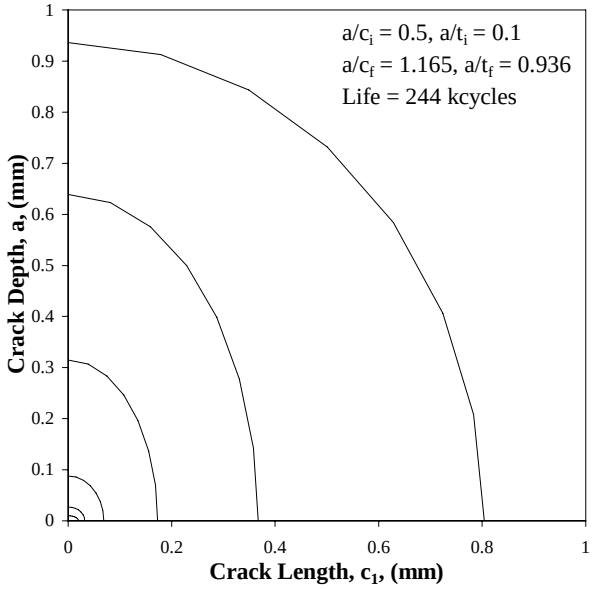

Figure 4 Crack Shape Development with Initial $a/c_1 = 0.5$

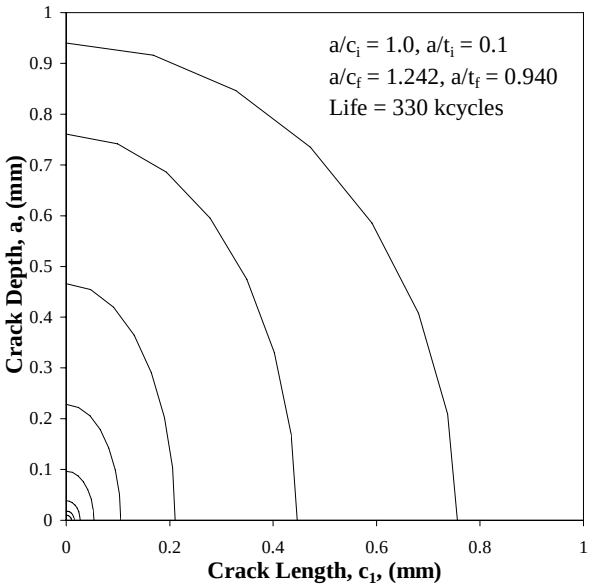

Figure 5 Crack Shape Development with Initial $a/c_1 = 1.0$

Although the initial a/c_1 ratios are highly different in the three figures, the final a/c_1 are similar but slightly increasing ($1.165 \le a/c_1 \le 1.338$) with the initial a/c_1 ratios. In [1], the final a/c_1 ratios calculated were constant at $a/c_1 \approx 0.575$. Since then, modifications to the Newman/Raju equations for a double corner crack at a hole have resulted in more continuous solutions for $a/t < 0.2$ and $a/t > 0.8$.[7,8] The figures show that the crack shape is always changing. The change in crack shape, a/c_1, is also evident in Figure 7 for each of the initial crack shapes, $a/c_1 = 0.5$, 1.0, and 2.0. Crack growth appears to be very much similar during the fatigue life, as should be expected, although the shape is changing. The final crack shape is converging to an $a/c_1 \approx 1.25$. The large difference in fatigue lives until break through may suggest a strong dependence on the initial flaw shape assumption. However, in Table 1, the life is split into an initial part until $c_1 = 0.25$ mm and a second part from $c_1 = 0.25$ to break through. It then turns out that the relatively large initial part of the life is strongly depending on the initial crack shape. A t the end of this initial part, the crack shapes for the three initial a/c_1 values are no longer that much different. As a consequence, the second part is practically independent on the initial crack shape. It has also been noted in the literature that semi-elliptical surface cracks with highly different a/c_1 values of the initial flaw show a tendency to grow to crack shapes with approximately the same a/c_1 ratio. Ichsan recently discussed this.[9] However, the results of the semi-elliptical surface cracks were grown under cyclical tension, which resulted in stabilized a/c_1 ratios close to 1.0. The present observation of a continually changing a/c_1 ratio for different initial flaw shapes is related to the occurrence of combined tension and bending.

The effect of the applied stress, specifically the ratio between the tension and bending stress, should be important. A similar parametric study was conducted using the same specimen dimensions as before except the initial flaw shape and size is fixed, $a_i = 0.2$, $c_i = 0.2$, and the bending factor, k ($=\sigma_b/\sigma_t$) is varied from 0 to ∞. As can be seen from Figure 8 and Table 2, as the bending factor increases, the a/c_1 ratio at break through decreases. This behavior is expected because increasing bending is increasing the stress at one side of the sheet and decreasing the stress at the opposing surface. In addition, the effect of the bending stress is also seen when comparing the fatigue lives of two cases where the maximum stress is the same. For example, for a σ_{max} = 150 MPa, the larger k (more bending) the longer the life, ≈305 compared to ≈116 kcycles.

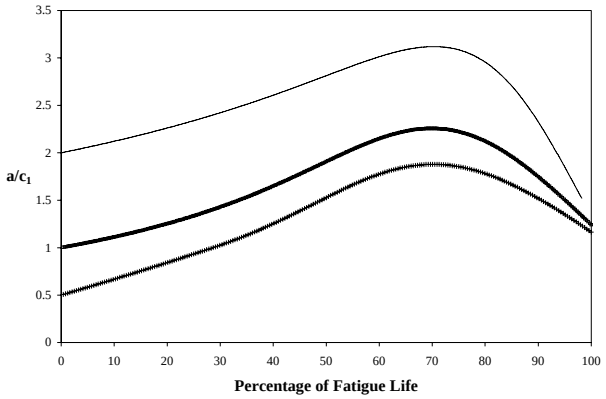

Figure 7 Crack Shape Development during the Fatigue Life

TABLE 1. Crack Growth of Initial Small Corner Flaws of Different Shapes until Break Through

Initial Flaw Data							Final Flaw Data						Crack Growth Life (kcycles)	
r/t	$a/c_1\|_i$	$a/t\|_i$	a_i (mm)	c_{1i} (mm)	$K_i(a)$ MPa√m	$K_i(c_1)$ MPa√m	$a/c_1\|_f$	$a/t\|_f$	a_f (mm)	c_{1f} (mm)	$K_f(a)$ MPa√m	$K_f(c_1)$ MPa√m	Life from initial flaw to $c_1 = 0.25$ mm	Life from $c_1 = 0.25$ mm to break through
1	0.5	0.01	0.01	0.02	2.389	2.125	1.165	0.936	0.936	0.804	7.306	9.926	176	68.0
1	1	0.01	0.01	0.01	1.951	1.752	1.242	0.940	0.940	0.756	7.114	9.579	262	67.9
1	2	0.01	0.01	0.005	1.538	1.151	1.338	0.943	0.943	0.705	6.888	9.207	535	67.8

3.2 Crack Extension Predictions along the Entire Crack Front

In the previous section, the crack extension was predicted for the ends of the two semi-axis, a and c_1, to arrive at the new crack front, assuming that it would remain quarter-elliptical. The Newman/Raju K-solution allows a calculation of K along the entire crack front. It implies that crack extension can be predicted for many points of the crack front. It leads to many new points of the moving crack front, which then can not be expected to be accurately a quarter elliptical curve with the same axes. However, it is possible to draw such a quarter ellipse through the new data points by adopting a regression analysis. The Newman/Raju equations can then be applied again for predicting the next crack extension. Ichsan adopted this procedure for a semi-elliptical surface crack loaded under remote tension only. He found that fitting an elliptical crack front for 32 points leads to a slightly longer fatigue life than predicted by the method of the previous section, i.e. predicting Δa and Δc_1 for the axes and assuming that the crack front remains elliptical. The difference was on the order of 10%. A similar comparison is made in [1] for two corner cracks at a hole under remote tension and bending (bending factor, k = 1) with similar results. Using more than 32 calculation points along the crack front results in a negligible effect on the fatigue life. However using fewer calculation points results in a slightly larger difference between the curve fit and non-curve fit prediction. The crack growth for the fit data is less than the unfit since the linear regression is decreasing the a or c_1 dimension by a small amount after each cycle. As can be expected, the small systemic decrease in crack size has a cumulative effect. As a result, a prediction with a small initial flaw assumption will undergo more regression calculations thereby having a larger effect on the fatigue life. To eliminate the systemic error due to curve fitting, at least 32 calculation points should be used.

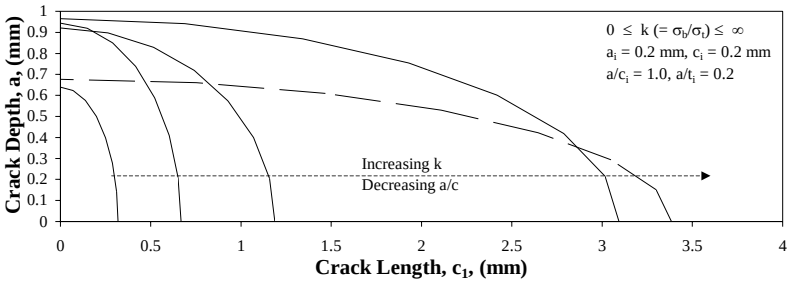

Figure 8 Crack Shape Development as a Function of the Bending Factor, k

TABLE 2 Dependence of Crack Shape on Bending Factor, k

k	σ_t (MPa)	σ_b (MPa)	σ_{max} (MPa)	$a/c_1\|_f$	$a/t\|_f$	life (kcycles)
0	100	0	100	2.000	0.640	120.923
0.5	100	50	150	1.411	0.943	116.494
1	100	100	200	0.775	0.920	75.277
2	50	100	150	0.312	0.965	304.515
∞	0	100	100	0.200	0.677	2086.260
	= a/c out of limits					

3.3 Comparison between Predicted and Observed Crack Shapes

Since in situ crack shape measurement is not currently possible, the only method of verifying the K solutions is by using the fatigue life or crack front shape after failure. For the 7-open hole tests, shown in Figure 9, several specimens were statically loaded to failure prior to failure by fatigue, and the crack shapes were measured. Thus for a given number of cycles, the crack shape is known and comparisons can be made with the analytical predictions. Such a comparison is shown in Figure 10 for five separate cracks in the same specimen. The predictions are completed assuming each hole is located in a finite width strip with no interaction with adjacent cracks. Since the cracks are still small, this procedure should be allowed. The five cracks do not have the same dimension because the initiation has taken different numbers of cycles. The shapes are predicted for the crack length "c_1" as observed, starting from a quarter elliptical crack with $a/c_1 = 1.0$. The initial a/c_1 value is not very important for the present size of the crack as discussed in section 3.1. Figure 10 shows a very good agreement with the crack shape development as observed from the specimen fracture surface. Similar satisfactory results were obtained for specimens with a single open hole also loaded by combined tension and bending.

4. The Growth of Through Cracks

The only K-solution for through cracks under combined loading conditions now available is the library of the NASGRO Fatigue Crack Growth Computer Program.[3] It applies to the loading cases shown in Figure 11. It assumes that the crack has a crack front perpendicular to the sheet surface. Predictions with these K-solutions are compared in section 4.1 to the test results presented in [1]. The effect of the initial flaw shape assumption and the bending factor on oblique through crack growth are discussed in section 4.2. In sections 4.3 and 4.4, the K-solutions developed in [1] are used.

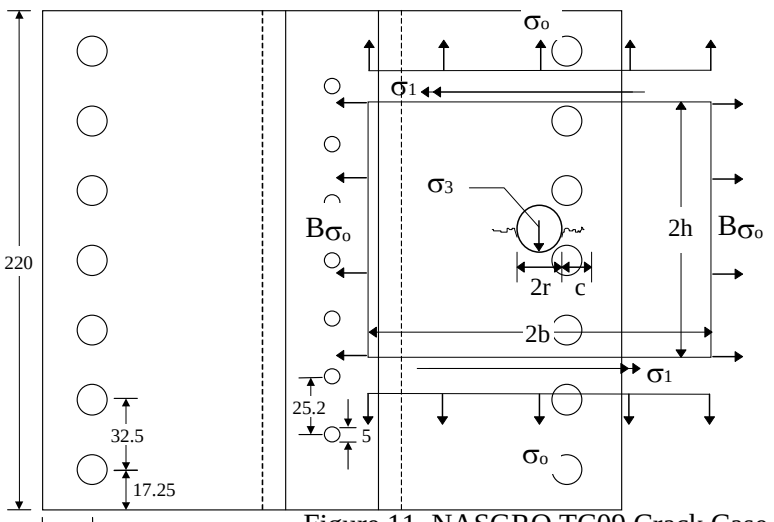

Figure 11 NASGRO TC09 Crack Case

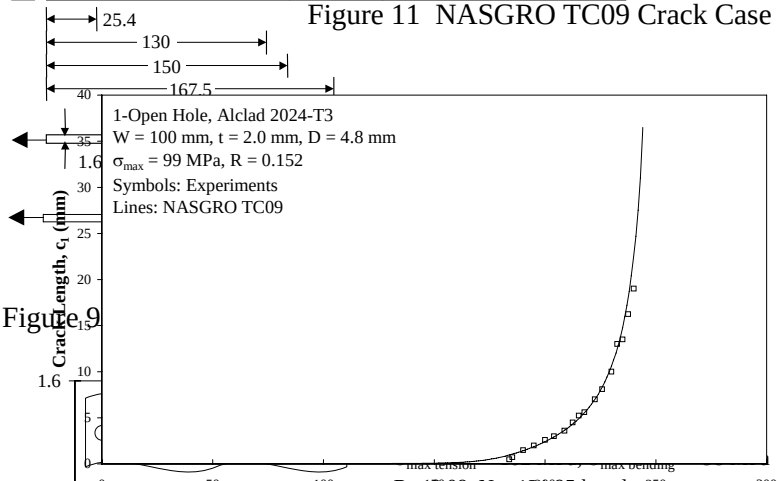

Figure 12 TC09 Verification Remote Tension

4.1 Through Crack Growth:
Published Stress Intensity Solutions

First predictions with the NASGRO K-solutions are made for through cracks starting from an open hole in a specimen loaded under tension only. An assumption had to be made about the crack initiation life, which was made to predict not only the fatigue life, but also the entire crack history. To do so an initial flaw size is assumed for which a prediction is made. A comparison is then made between the actual and predicted crack histories. If the prediction is underestimating the crack growth, the initial flaw size is increased; conversely, if the prediction is overestimating the crack growth, the initial flaw size is decreased. An example of the comparison between prediction and tests results is shown in Figure 12, which shows a good agreement. Similar correlation was obtained for all open hole specimens loaded by remote tension only.

Unfortunately, the correlation is not as good for specimens subject to combined remote tension and bending shown in Figure 13. Crack growth rates for cracks larger than 2 mm are highly overestimated. Although some aspects of the theoretical background of the NASGRO K-solutions may be questioned, there is one obvious reason for disagreement. In the NASGRO concept, the crack is supposed to be a

through crack with a straight crack front perpendicular to the plate surface. In reality, under combined tension and bending such cracks grow with an oblique part-elliptical front. In Figure 13, the crack length plotted is c_1 (see Figures 1 and 3), which is the largest length of the crack at the material surface where the bending stress has its maximum. Since the crack through the thickness is lagging behind this point the cracked area is smaller than assumed in the NASGRO solution. An overestimation of the crack growth should then be expected.

4.2 The Effect of the Initial Flaw Shape a/c_1

A similar parametric study conducted for the part-through cracks is done for the oblique through cracks (OTC). For the predictions that are completed here, an initial crack length, c_1 = 2.1 mm, has been used with four values of the a/c_1 ratio: 0.5, 1.0, 1.5, and 2.0, i.e. a = 1.05, 2.1, 3.15, and 4.2 mm, respectively. The calculations are for a 100 mm wide specimen of 2024-T3, thickness 1.0 mm with a 2.0 mm hole in the center. The remote stress is 100 MPa of both tension and bending (bending factor k = 1.0). Results are shown in Figure 14 - Figure 17 for the four a/c_1 ratios, respectively. The figures show crack fronts obtained at intervals of approximately 20% of the fatigue life. The last crack front applies to net section yield or $K_{applied}(c_1) > K_{Ic}$.

Although the initial a/c_1 ratios are highly different in the four cases, the final a/c_1(=0.435) are exactly the same. Similarly, the final a/t (=2.175) ratios are the same for all four predictions. Generally, the magnitude of K for a straight through crack from a hole is larger than an OTC of the same c_1 length. This behavior is manifest in the slightly larger fatigue life for the crack, Figure 14, with initially high a/c_1 and a/t ratios. Figures 14 – 17 as well as Figure 18 shows that the crack shape quickly stabilizes regardless of the initial shape. In view of the difficulties in accounting for the crack shape during the transition between a part through crack to OTC, it appears that assuming an "incorrect" shape for the first cycle as an OTC is of little consequence. Recall, when the part through crack breaks through the thickness there is an instantaneous increase in the crack depth and most likely no noticeable increase in the crack length; thus a crack shape must be assumed for the beginning of the OTC portion of the prediction.

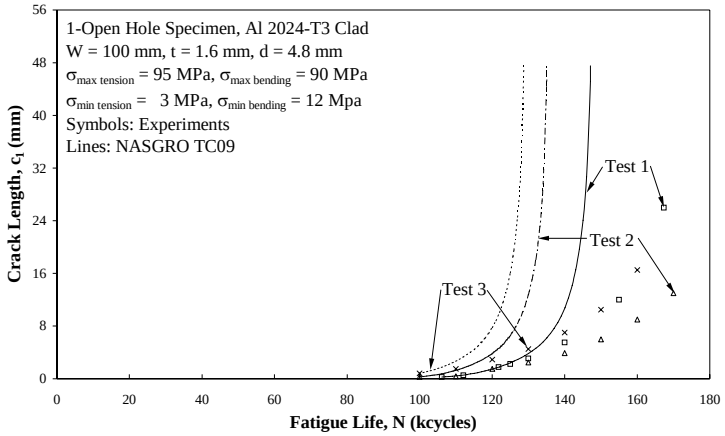

Figure 13 TC09 Verification Remote Tension and Secondary Bending

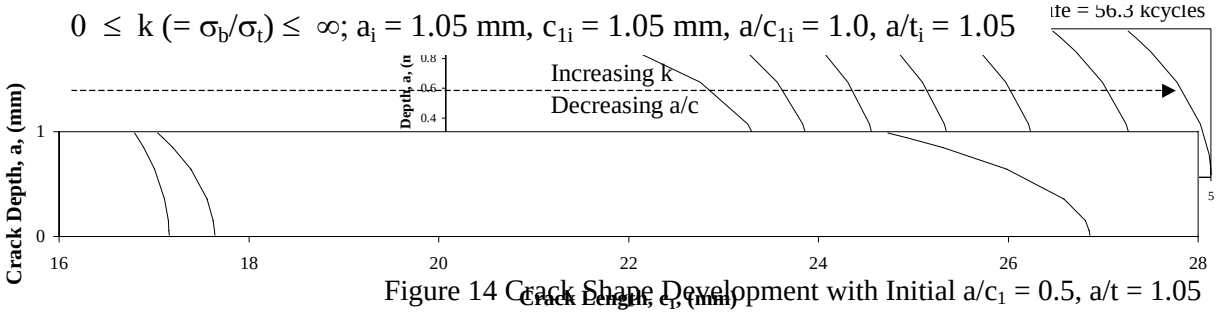

Figure 14 Crack Shape Development with Initial $a/c_1 = 0.5$, $a/t = 1.05$

Figure 19 Effect of the Bending Factor, k on Flaw Shape Development

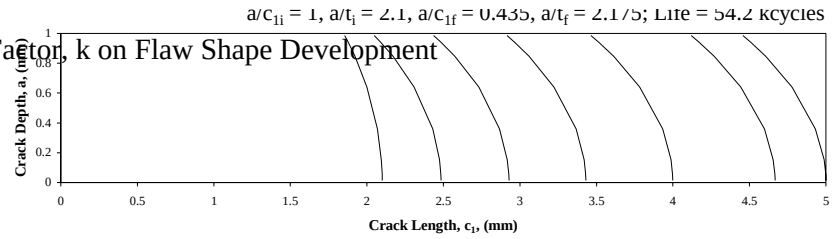

Figure 15 Crack Shape Development with Initial $a/c_1 = 1$, $a/t = 2.1$

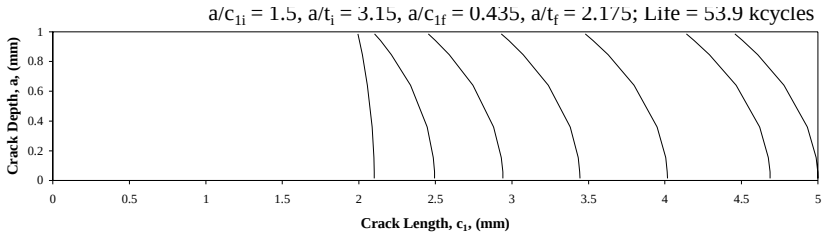

Figure 16 Crack Shape Development with Initial $a/c_1 = 1.5$, $a/t = 3.15$

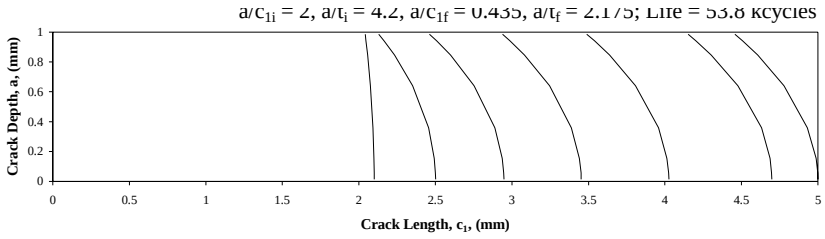

Figure 17 Crack Shape Development with Initial $a/c_1 = 2$, $a/t = 4.2$

In the parametric study above, it was shown that the initial flaw shape assumption is of little consequence in fatigue life predictions. Furthermore, the effect of the applied stress, specifically the ratio between the tension and bending stress, should be important. A similar parametric study was conducted using the same specimen dimensions as before except the initial flaw shape and size is fixed, $a_i = 1.05$, $c_{1i} = 1.05$, and the bending factor, k ($=\sigma_b/\sigma_t$) is varied from 0.5 to 2.0. As can be seen from Figure 19 and Table 3, as the bending factor increases, the a/c_1 ratio decreases. This behavior is expected for the same reason as stated for the part through cracks, the larger k (more bending) the smaller the a/c_1 and longer the life, ≈754 compared to ≈205 kcycles.

TABLE 3 Dependence of Crack Shape on Bending Factor, k

k	σ_t (MPa)	σ_b (MPa)	σ_{max} (MPa)	$a/c_1\|_f$	$a/t\|_f$	Life (kcycles)
0.5	100	50	150	0.280	4.809	204.685
1	100	100	200	0.216	3.810	131.932
2	50	100	150	0.094	2.527	754.256

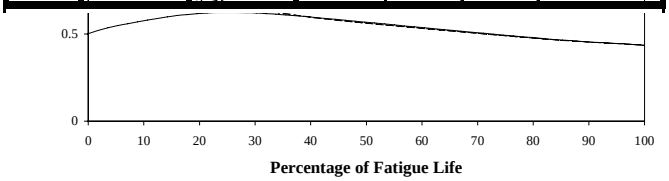

Figure 18 Effect of Initial Flaw Shape on Flaw Shape Development

4.3 Through Crack Growth Predictions with the New K-Solutions: Open Hole Specimens

K-solutions for oblique through cracks at a hole were obtained from finite element analyses for a range of crack depth to crack length ratios ($a/c_1 = 0.2, 0.3, 0.4, 0.6, 1.0, 2.0$), crack depth to sheet thickness ratios ($a/t = 1.05, 1.09, 1.13, 1.17, 1.21, 2.0, 5.0, 10.0$) and hole radius to sheet thickness ratios ($r/t = 0.5, 1.0, 2.0$).[1] The results were presented in tabular format. These values could be converted to a polynomial

description of the results. However, with the computational power of current desktop personal computers, there is no need for the time consuming derivation of such polynomial equations. A computer program has been developed, which by interpolation obtains the K-values for the applicable crack shape and size, defined by values of a/c_1, a/t, and r/t. The interpolation is handled by a choice of three different interpolation routines; linear, higher order polynomial, or cubic spline. Although the linear interpolation is attractive in it's simplicity, it is not well suited for interpolating between the large ranges in the a/c_1 and a/t values. Both the higher order polynomial and cubic spline routines are used with no distinguishable difference. However, the cubic spline appears to be more stable than the higher order polynomial in extrapolating K's from a table. Extrapolation may be required in a/c_1 in the latter stage of the fatigue life where the crack is growing quite rapidly, and the crack front is straightening out resulting in large a/c_1 ratio.

The new K solutions have been used to predict the fatigue life of an open hole specimen subject to tension and bending ($k \approx 1.0$). The cracks nucleate and grow naturally as corner cracks; thus, the Newman/Raju K-solution is used until the crack grows through the thickness of the sheet. Once the crack is a through crack, the new solutions are used until final fracture.

The transition from a part through to through crack is difficult to examine experimentally; therefore an assumption of the transition behavior was made as explained previously in section 1. Examination of the fracture surfaces of the fatigue specimens that were statically overloaded to failure when the crack was close to the transition area did not show a detectable change in the crack shape. As mentioned previously, since the fracture surfaces must be viewed by destructive inspection, the comparison is made of cracks from different specimens of the same geometry tested at the same remote stress level. Thus, the factor of 1.05 does not alter the crack shape significantly, but does account for the instantaneous increase in the crack depth at the moment of break through. Additional assumptions that must be made in the prediction calculation are the initial flaw size and shape. Based on fractographic observations, the initial crack shape is assumed to be quarter circular, $a/c_1 = 1.0$. The initial flaw size is estimated. The prediction algorithm iterates by varying the initial flaw size (quarter circular shape) until the crack length and number of cycles at failure is achieved.

The prediction of the open hole specimen subject to combined tension and bending shown in Figure 20 does not exactly follow the entire crack growth history. The transition from a part through to a through crack is seen at approximately 112 kcycles where the crack length and depth (the latter not shown in the figure) is about 1.8 mm. The predictions previously reported in [1], showed a slight cusp in the prediction curve during the transition from a part through to a through crack. This was attributed to not accurately calculating K in the transition region. Specifically, the front surface K calculated for the last cycle as a part through crack is higher than the first K calculated for the through crack, implying a higher crack growth rate just before break through. The ligament width in the thickness direction is going to zero and such a behavior might occur in view of the questionable K-values at the moment of the transition. Grandt et al. reported a nearly constant crack

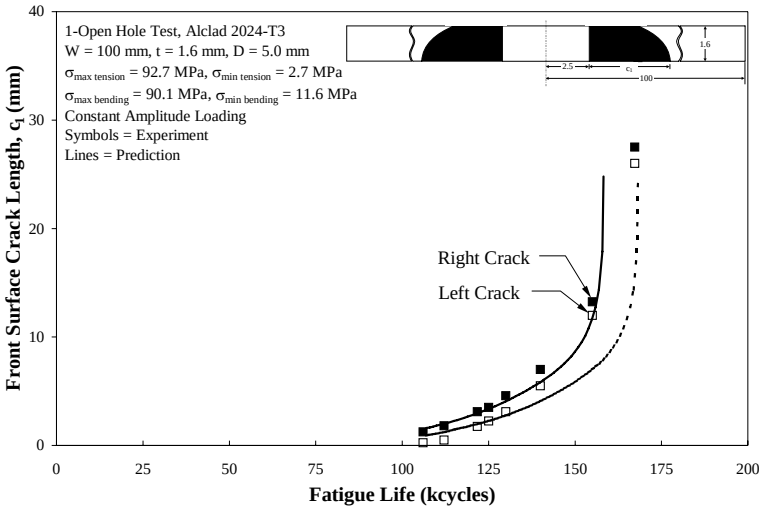

Figure 20 Crack Growth Prediction in 1-Open Hole Specimen Subject to Combined Tension and Bending

growth rate for the c_1 crack length during the transition from a part through to through crack.[10] As seen in Figure 20, the cusp in the transition region has disappeared which is attributed to using the modified Newman/Raju equations.[7,8]

The new K's do not account for a changing stress field, which occurs as the crack becomes quite long. A long crack implies a reduction in the bending stiffness of the sheet; thus, the crack is experiencing a more tensile stress field. In a tension dominant stress field, it was shown in [1] for a center cracked sheet with a part elliptical oblique crack subject to pure tension and separately combined tension and bending that the K's for the pure tension case are higher than that for the combined loading assuming the same applied remote stress. From the correlation between actual and predicted crack histories in Figure 20, the K solutions used for this complex crack shape subject to combined tension and bending loading are reliable. Within the scope of linear elastic fracture mechanics, K remains to be a good similitude parameter when the crack geometry and loading condition are well characterized.

4.4 Through Crack Growth Predictions with the New K-Solutions: Asymmetric Lap-Splice Joint Specimens

The asymmetric lap-splice joint shown in Figure 21 was fatigue tested using a program loading spectrum that creates marks, groups of fatigue striations, on the fracture surface which can be clearly seen at low magnification (typically less than 5000X) in the scanning electron microscope. The spectrum is composed of blocks of constant amplitude loading followed by smaller blocks of constant amplitude loading at a lower K_{max} and was successfully used by Piascik[11] and Fawaz[1]. The joint offers several simplifying features when compared to lap-splice joints used in transport aircraft in that the load transfer in each rivet row is known, 50%, and the joint has a point of symmetry at its centroid. The K-calculations include tension, bending, and hole loading.

Predictions for the asymmetric lap splice joint are shown in Figure 22 and 23. As was discussed in section 3.1, the initial flaw size and shape strongly affect the fatigue behavior of small cracks. Attempts have been made to try and predict the small crack history when the crack is still a corner crack using the Newman/Raju solution. However, since the flaw shape at these small crack lengths cannot be determined from the marker bands, predictions are made for several initial flaw shapes (a/c_1 = 0.2, 1.0, 1.5, and 2.0) using the known c_1 crack length. From these predictions, the initial flaw shape did not affect the crack shape at break through which was previously shown in Figure 4 - 6. Even though the life to break through slightly increases with a larger initial a/c_1, the Newman/Raju solutions do adequately predict crack growth of an initial crack to break through. Note Figure 22 is for a crack that has not grown through the thickness. It is worth noting that the Newman/Raju solutions do not account for rivet interference or load transmission by friction between the sheets at the faying surface, both of which can result in decreasing the load available for crack extension. Since a low squeeze force was used to install the rivets, the hole expansion and clamping force are low diminishing the residual stresses near the rivet hole. In a joint with highly squeezed rivets, the predictions may not

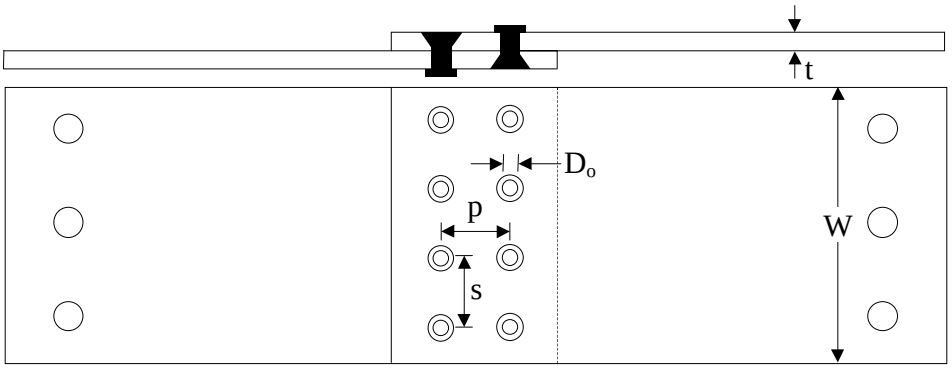

Figure 21 Asymmetric Lap Splice Joint

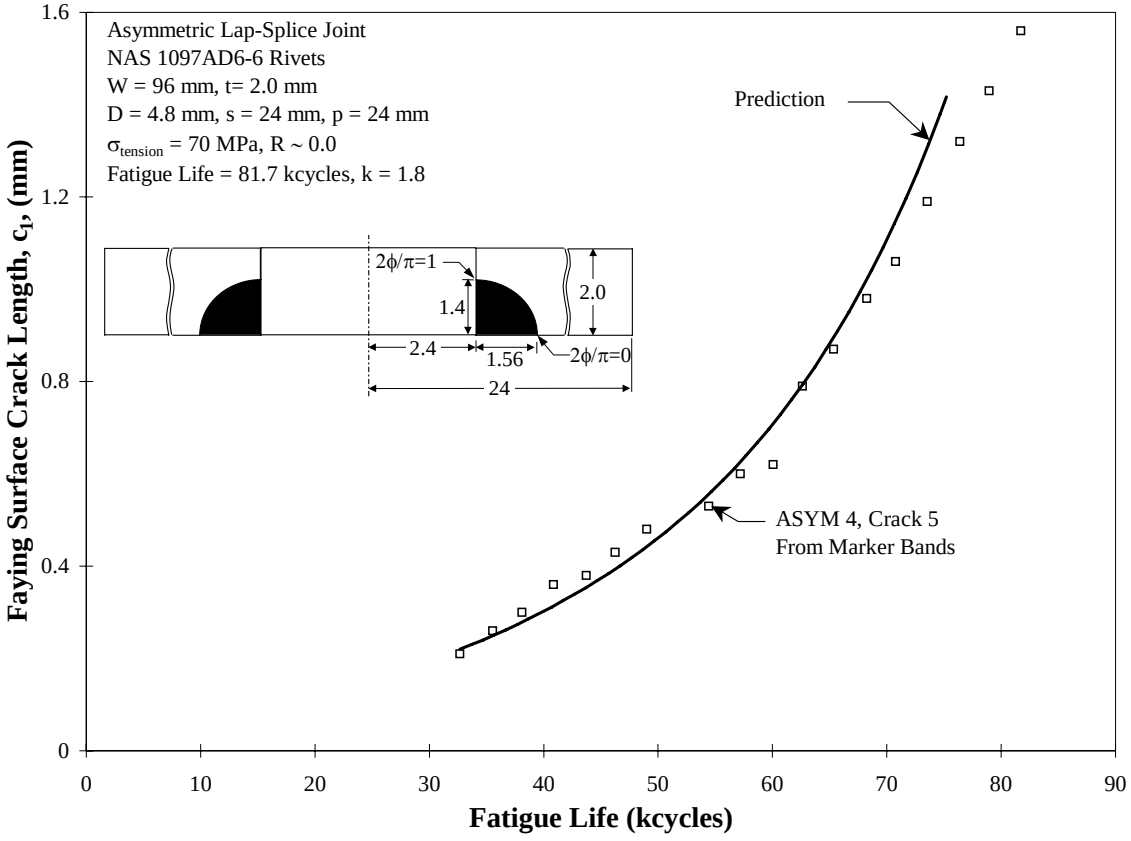

Figure 22 Crack Growth Prediction for Asymmetric Lap Splice Joint, Part Through Crack

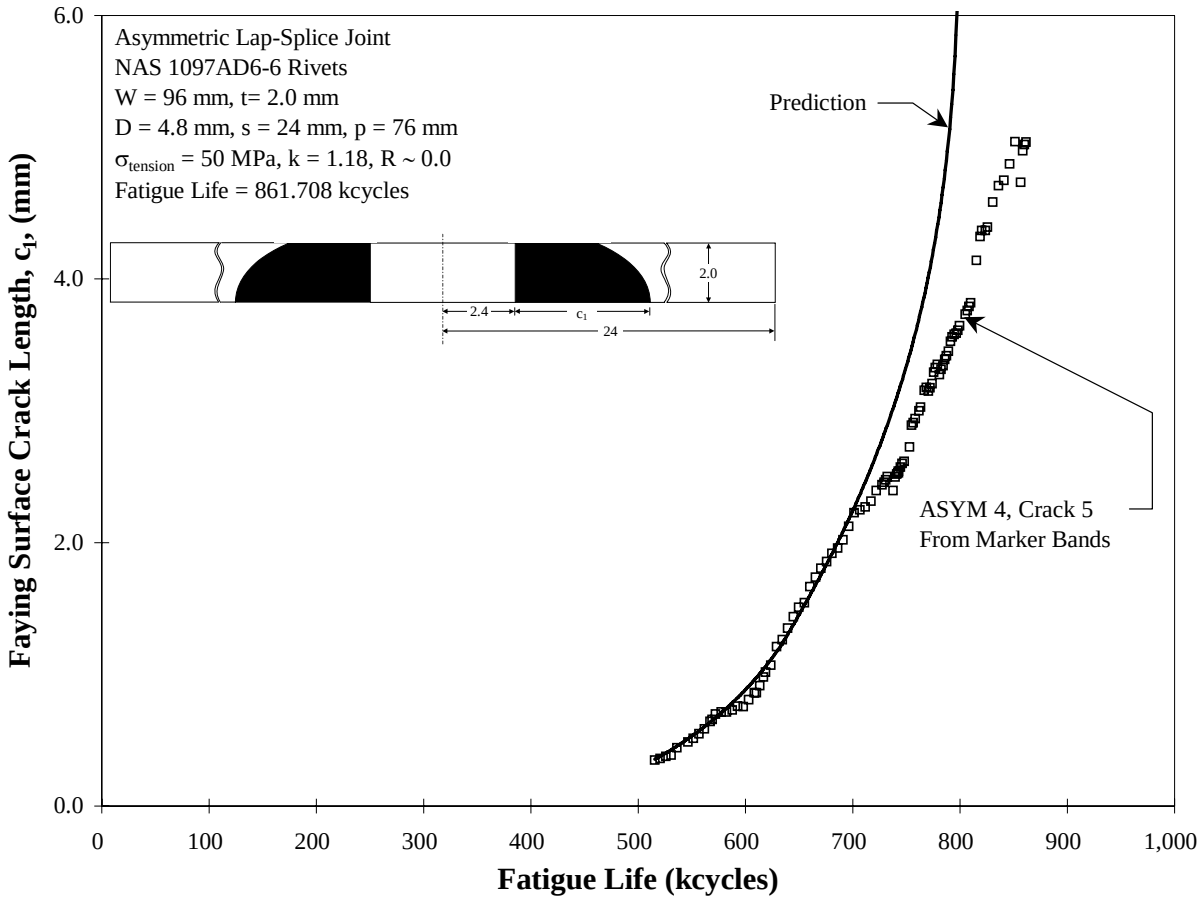

Figure 23 Crack Growth Prediction for Asymmetric Lap Splice Joint, Through Crack

correlate to the test data as well. In that case then, a shortcoming in the prediction model would be the inability to account for interference and load transmission by friction. The prediction in Figure 23 as well as that shown in Figure 22 shows the new K solutions are performing reasonably well. In Figure 23, the prediction underestimates the fatigue life by approximately 10% resulting from a slight overestimation of K during the through crack portion. Examination of the fracture surface of both critical rows showed extensive cracking. As adjacent cracks grow, the rivet is less effective in transferring the load; thus, the load is redistributed to the remaining rivets. Not accounting for load shedding is another weakness of the model. By the rather steep slope of the through crack region, the crack is growing quite fast with slightly more than 10% of the fatigue life remaining. Assuming the crack is growing from a rivet hole in a finite width sheet with no other cracks at other rivets is an oversimplification of the cracking scenario.

5. Conclusions

- Crack Growth Prediction Methodology: da/dN - ΔK Relation
  - In general, the same crack growth prediction methodology developed and used in the NASGRO Crack Growth Computer Program is adopted. The Forman-Newman-de Koning crack growth law is available in the crack growth prediction computer program, but due to the simplicity of the load spectrum (CA) and the well characterized sheet material (2024-T3), the FNK equation is degenerated to the closure corrected Paris Law for all predictions.
- Crack Growth Predictions Using Published K Solutions

- Double Corner Cracks at a Hole Subject to Tension and Bending, Newman/Raju
  - The Newman/Raju solutions accurately predicted both the crack shape and fatigue life for open hole specimens subject to remote tension and bending, (Figure 10).
  - The initial flaw shape assumption has a negligible effect once the crack length at the material surface, "c_1" exceeds 0.25 mm in a 1.0 mm thick sheet. However, due to the dependence of the K-value at the material surface, $K(c_1)$, on the "c_1" crack length, crack growth in the small crack regime ($c_1 \leq 0.25$ mm) is affected.
  - For studying the K variation along the crack front, a regression analysis must be preformed after each crack growth increment to fit the crack front back to an elliptical shape. To avoid regression analysis errors with the N/R solutions, 32 calculation points along the crack front must be used. Otherwise systematic errors occur in the crack shape (either in the crack depth or crack length) ultimately affecting the fatigue life.
- Double Through Cracks at a Hole Subject to Tension and Bending (NASGRO TC09)
  - The TC09 solution accurately predicted crack growth in open hole specimens loaded in pure tension (Figure 12), but underestimated the fatigue life consistently by at least 30% for combined tension and bending (Figure 13).

- Crack Growth Predictions with Newly Developed K Solutions
  - The new K solutions for two part-elliptical, oblique through cracks at a hole have been used to predict the fatigue life of an open hole specimen subject to combined tension and bending ($k \approx 1.0$). In addition, predictions have been completed for an asymmetric lap splice joint.
  - Predictions of the *open hole* specimens subject to combined tension and bending ($k \approx 1$) show good agreement for a majority of the crack history. The predicted crack size is underestimated in the last 6% of the fatigue life.
  - Predictions of the *asymmetric lap-splice joint* are also adequate with the fatigue life being underestimated for both reconstructed crack histories, Figure 22 and 23. If crack growth in riveted joints is to be predicted more accurately, consideration of the effects of friction and residual stresses on the part through crack growth and crack interaction on the through crack growth is required.

REFERENCES

[1] Fawaz, Scott Anthony. Fatigue Crack Growth in Riveted Joints. Diss. Delft University of Technology, 1997. Delft, NL.

[2] Forman, Royce G., Vankataraman Shivakumar, James C. Newman Jr., Susan M. Piotrowski, and Leonard C. Williams. Development of the NASA/FLAGRO Computer Program. Fracture Mechanics: Eighteenth Symposium ASTM STP 945. D. T. Read and R. P. Reed, Eds., American Society for Testing and Materials, Philadelphia, 1988. 781-803.

[3] NASGRO Fatigue Crack Growth Computer Program, Version 2.01, NASA JSC-22267A, 1994.

[4] Forman, R. G., and S. R. Mettu. Behavior of Surface and Corner Cracks Subjected to Tensile and Bending Loads in Ti-6Al-4V Alloy. Fracture Mechanics: Twenty-Second Symposium, Vol. 1, ASTM STP 1131, H. A. Ernst, A. Saxena, and D. L. McDowell, Eds., American Society for Testing and Materials, Philadelphia, 1992. 519-546.

[5] Newman Jr., J. C. "Crack Opening Stress Equation for Fatigue Crack Growth," International Journal of Fracture. 24 (1984): R131-R135.

[6] Newman, Jr., J. C. and I. S. Raju. Stress Intensity Factor Equations for Cracks in Three-Dimensional Finite Bodies Subjected to Tension and Bending Loads. NASA-TP-85793, 1985.

[7] Zhao, W., J. C. Newman, Jr., M. A. Sutton, X. R. Wu, and K. N. Shivakumar, "Analysis of Corner Cracks at Hole by a 3-D Weight Function Method with Stresses from Finite Element Method," NASA Technical Memorandum 110144, July 1995.

[8] Zhao, W. and Newman, Jr., J. C., Electronic Communication, Unpublished NASA Langley Research Center Results, 24 February 1998.

[9] Putra, Ichsan, S. Fatigue Crack Growth Predicitons of Surface Cracks Under Constant-Amplitude and Variable-Amplitude Loading. Diss. Delft University of Technology, 1994. Delft:NL.

[10] Grandt, Jr., A. F., J. A. Harter, and B. J. Heath, "Transition of Part-Through Cracks at Holes into Through-the - Thickness Flaws," Fracture Mechanics: Fifteenth Symposium, ASTM STP 833, R. J. Sanford, Ed., American Society for Testing and Materials, Philadelphia, 1984, pp. 7-23.

[11] Piascik, Robert S. and Scott A. Willard. The Characterization of WideSpread Fatigue Damage in the Fuselage Riveted Lap Splice Joint. NASA-TP-97-206257, 1997.